

Characterization of the International Linear Collider damping ring optics

J. Shanks, D.L. Rubin, and D. Sagan

CLASSE, Cornell University, Ithaca, New York 14853, USA
js583@cornell.edu

ABSTRACT: A method is presented for characterizing the emittance dilution and dynamic aperture for an arbitrary closed lattice that includes guide field magnet errors, multipole errors and misalignments. This method, developed and tested at the Cornell Electron Storage Ring Test Accelerator (CesrTA), has been applied to the damping ring lattice for the International Linear Collider (ILC). The effectiveness of beam based emittance tuning is limited by beam position monitor (BPM) measurement errors, number of corrector magnets and their placement, and correction algorithm. The specifications for damping ring magnet alignment, multipole errors, number of BPMs, and precision in BPM measurements are shown to be consistent with the required emittances and dynamic aperture. The methodology is then used to determine the minimum number of position monitors that is required to achieve the emittance targets, and how that minimum depends on the location of the BPMs. Similarly, the maximum tolerable multipole errors are evaluated. Finally, the robustness of each BPM configuration with respect to random failures is explored.

KEYWORDS: Accelerator modelling and simulations (single-particle dynamics); Beam Optics.

Contents

1. Introduction	1
2. DTC04 Lattice	3
3. Misalignment and Correction Procedure	4
4. Error Tolerance of DTC04	7
4.1 Nominal Lattice and Errors	7
4.2 Reduced BPM Schemes	8
4.3 Effect of Random BPM Failures	11
5. Dynamic Aperture	11
6. Summary and Future Work	13
Appendix: DTC04 Magnet Misalignments and Multipoles	14

1. Introduction

The International Linear Collider (ILC) design utilizes damping rings to cool beams delivered by the electron and positron sources before transferring to the main linacs [1]. Three of the primary requirements of the baseline damping rings are: 1) they must accept an injected bunch from the positron source with normalized phase-space amplitude $0.07 \text{ m} \cdot \text{rad}$ and $\delta_E/E = 0.75\%$; 2) the beams must be cooled to an equilibrium zero-current geometric vertical emittance $\leq 2 \text{ pm}$; and 3) the damping time must be short enough to provide fully damped bunch trains at a repetition rate of 5Hz.

The above requirements must be met in a real machine that includes magnet misalignments, guide field multipole errors (both systematic and random), and beam position monitor (BPM) measurement errors. Emittance tuning will be essential to achieve the target zero-current emittance. Quadrupoles and corrector magnets will necessarily be independently powered, allowing for localized corrections through the use of beam-based measurements.

The damping rings cannot be characterized with respect to the exact set of errors they will have, as the rings are not yet built. For the purposes of this study, alignment errors in the damping rings are assumed to be randomly distributed with amplitudes dictated by survey tolerances. By simulating a large number of lattices with random distributions of errors at the appropriate levels, the damping rings can be characterized with a statistical analysis of the likelihood that the required emittances and dynamic aperture will be achieved. A configuration is deemed acceptable if 95% of

the randomly-misaligned and corrected lattices meet the required vertical emittance and dynamic aperture, as per the Technical Design Report specifications.

Several methods for optics correction have been developed at storage ring light sources. By far the most widespread method is response matrix analysis (RMA), and specifically, orbit response matrix (ORM) analysis [17]. The method involves taking difference orbits where corrector strengths are varied. Both the Swiss Light Source and Australian Synchrotron have demonstrated the capability of correcting vertical emittance below 1 pm using ORM [3, 9], below the required vertical emittance for the ILC damping rings. However, the time required for ORM data acquisition scales linearly with the number of correctors in the ring. For large rings such as the proposed ILC damping rings with over 800 steering correctors, acquiring difference orbits becomes a time-consuming process.

Another increasingly-common class of optics correction algorithms is based on turn-by-turn BPM measurements, where the beam is pinged with a short-duration kick and allowed to oscillate freely [6, 2]. Typically this data is then processed as a resonance-driving term (RDT) correction [13]. This correction technique has the benefit that correction times are roughly independent of the size of the ring. For the ILC this represents a considerable savings in time. While this method has shown promise, there are limitations. The beam decoheres due to amplitude dependent tune shift, limiting the number of useful turns of data. The decoherence may be partially mitigated by reducing the chromaticity to near zero, however measurements are still limited to a few thousand turns. As mentioned in [2], the resolution of the betatron phase measurement scales roughly inverse with the number of turns ($1/N$). The limitations on the number of turns in a data set therefore directly correspond to a limitation on accuracy of betatron phase measurements.

A turn-by-turn-based alternative to RDT has been developed for use at the Cornell Electron Storage Ring (CESR) for CESR Test Accelerator program (CesrTA) [10, 22]. The CESR betatron phase and coupling measurement relies on phase-locking turn-by-turn kickers to resonantly excite a single bunch to an amplitude of several millimeters, thus avoiding limitations due to bunch decoherence and allowing for data sets of over 40,000 turns. The effectiveness of the betatron phase/coupling correction procedure has been evaluated at CesrTA through measurements and simulations, demonstrating good agreement and validating our understanding of the limitations of optics correction.

In this paper, the method for modeling optics correction developed at CesrTA is used to characterize the ILC damping rings. Several scenarios are evaluated, including the possibility of reducing the total BPM count and relaxing the constraints on guide field multipole errors, with respect to the baseline design. The effect of random BPM failures is analyzed to benchmark the robustness of each of the proposed BPM distributions.

The characterization is comprised of two parts: generating a randomly misaligned lattice and simulating the optics correction procedure, and analyzing the dynamic aperture of the corrected lattice as a function of guide field multipole errors. The software used in all analyses is based on the Bmad accelerator code library [18].

Only single-particle dynamics from the beam optics are considered in the work presented here. The reported emittances therefore represent the zero-current limit. Other current-dependent sources of emittance dilution, such as intra-beam scattering (IBS), electron cloud, and fast-ion instability will increase the vertical emittance beyond this lower limit.

2. DTC04 Lattice

The baseline ILC damping ring design is the DTC04 lattice developed by Rubin *et al.* [21]. The lattice is a 3.2 km racetrack with a modified TME-type arc cell. The zero-dispersion straights are based on the work of Korostelev and Wolski [14]. A schematic of the ring is shown in figure 1. Optics functions are shown in figure 2. Tables 1 and 2 summarize the lattice parameters and number of magnets of each class. The quoted emittances $\epsilon_{a,b}$ are the horizontal-like and vertical-like normal modes, respectively. In the absence of coupling, these will correspond to $\epsilon_{x,y}$. Decomposition into normal modes is discussed elsewhere [25, 16, 4], and as such, a derivation is omitted here.

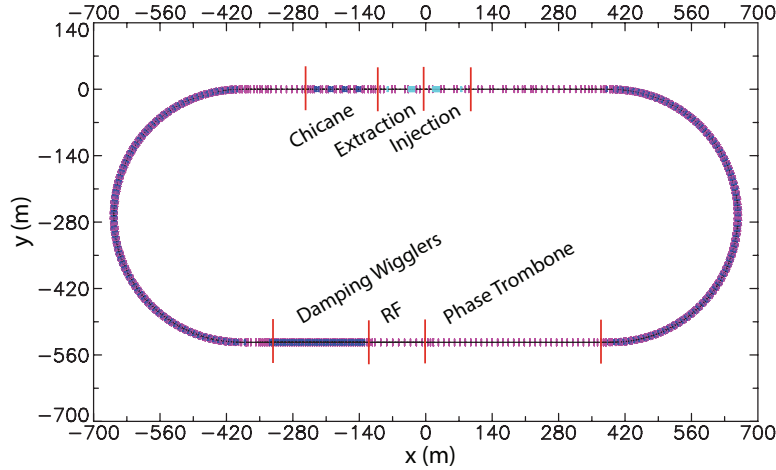


Figure 1: Layout of DTC04 lattice.

Table 1: Summary of the DTC04 lattice parameters.

Parameter	Value	Units
Circumference	3239	m
Energy	5.0	GeV
Betatron Tunes (Q_x, Q_y)	(48.850, 26.787)	
Tune Advance per Arc	(16.418, 6.074)	
Chromaticity (ξ_x, ξ_y)	(1.000, 0.302)	
Chromaticity per Arc	(9.074, 10.896)	
Train Repetition Rate	5	Hz
Bunch Population	2×10^{10}	
Extracted $\epsilon_a^{geometric}$	0.6	nm
Extracted $\epsilon_b^{geometric}$	< 2	pm
Extracted Bunch Length	6	mm
Extracted σ_E/E	0.11	%
Damping Time	24	ms
Wiggler B^{max}	1.5	T

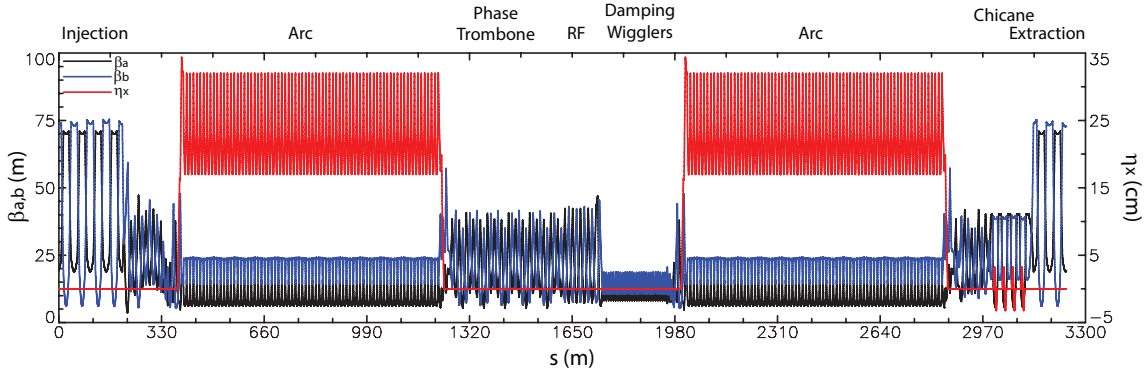


Figure 2: Horizontal and vertical β functions and horizontal dispersion for the DTC04 lattice. The ripple in β_b in the arcs is due to aliasing, and is not physical.

Table 2: Summary of elements in the DTC04 lattice.

Class	Count
Beam Position Monitor	511
Dipole	164
Horizontal Steering	150
Vertical Steering	150
Combined H+V Steering	263
Quadrupole	813
Skew Quadrupole	160
Sextupole	600
Damping Wigglers	54

The arc cell layout is shown in figure 3. Arc cells are comprised of one dipole, three quadrupoles, four sextupoles, one horizontal and one vertical steering corrector, one skew quadrupole, and two beam position monitors.

3. Misalignment and Correction Procedure

The effects of misalignments, BPM errors, multipoles, and choice of correction procedure are evaluated by the program `ring_ma2` [22]. The `ring_ma2` workflow is structured as follows:

1. Assign random misalignments and BPM errors with user-defined amplitudes to the ideal lattice to create a realistic machine model.
2. Simulate beam based measurements of optics functions including the effects of BPM measurement errors.
3. Compute and apply corrections for each iteration based on the simulated measurements.
4. After each correction iteration, record the effectiveness of the correction in terms of emittances and optics functions.

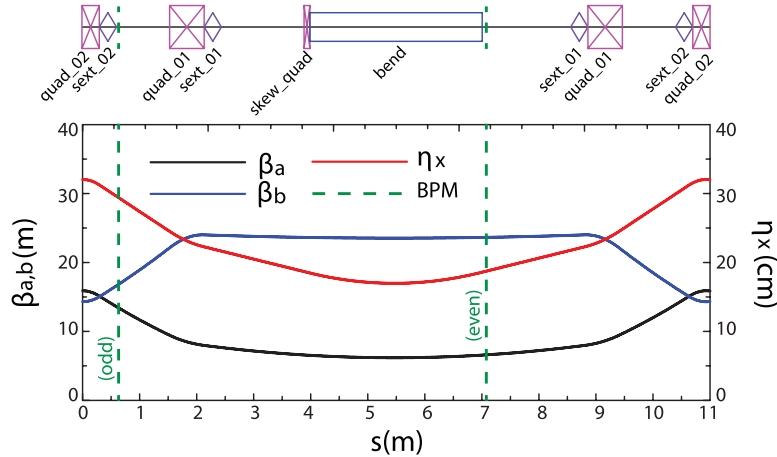


Figure 3: DTC04 arc cell. Two BPMs are available in each arc cell, and are either odd-indexed or even-indexed.

The entire procedure is repeated typically 100 times, each with a randomly chosen distribution of errors in order to generate statistics sufficient for analysis. Misalignments are allowed on any element parameter described by `Bmad`, including but not limited to: position offsets and angles, random field strength errors, and systematic and random multipole errors. BPM measurement errors allowed in the simulation include BPM-to-quadrupole transverse offset, tilt, button-by-button gain error, and button-by-button timing errors.

The particular configuration of the guide field magnets, correctors, and BPMs is referred to as a scenario. For each scenario, 100 lattices are generated with random errors and misalignments. Each misaligned lattice is referred to as a seed. As noted above, typically 100 seeds are used for the evaluation of each scenario, and the same 100 seeds are used when evaluating multiple scenarios. That is, for a given seed, each element in a lattice for each scenario starts with the same misalignments and field errors, regardless of whether a subset of elements or detectors are vetoed or disabled during the correction.

The method used for simulating measurements with BPM errors is based on the method developed for diagnosing emittance dilution at CesiTA [22]. In the original analysis, modeling the full correction procedure includes turn-by-turn tracking for several damping times in order to accurately simulate measurements of betatron phase and coupling. The turn-by-turn measurements are then post-processed identically to actual machine data into orbit, dispersion, or phase and coupling data. Though this method for simulation is as close to modeling the actual measurement process, it is very time-consuming. In the case of the ILC damping ring lattice, this method is prohibitively slow due to the large number of elements. Two modifications have been made to the measurement simulation procedure in order to improve the efficiency of the calculations such that the characterization method developed in [22] may be applied.

First, there is a modification to tracking in the damping wigglers. When accounting for wiggler nonlinearities is required, a fully-symplectic Lie map is used for tracking through the damping wigglers [7, 8]. However, as it is presently implemented in `Bmad`, this tracking method is computationally intensive. When the full nonlinearities of the damping wigglers are known to not affect the

resulting simulation, a simplified MAD-style “bend-drift-bend” wiggler model which preserves the radiation integrals can be used to reduce the time required for simulations. Radiation integrals and horizontal emittances the two wiggler models are shown in table 3. The horizontal emittances computed with the two models differ by less than 3%. The level of agreement is more than sufficient for the studies presented here.

Table 3: Comparison of emittance and radiation integrals for DTC04 lattice with two wiggler models: a fully-symplectic Lie map, and a simplified “bend-drift-bend” model.

Parameter	Lie Map	Bend-Drift-Bend	Δ
ϵ_a	0.553 nm	0.567 nm	-2.51%
I_1	1.08	1.08	0.00%
I_2	0.512 m^{-2}	0.515 m^{-2}	-0.59%
I_3	$3.39 \times 10^{-2} \text{ m}^{-3}$	$3.40 \times 10^{-2} \text{ m}^{-3}$	-0.44%
I_4	$1.98 \times 10^{-4} \text{ m}^{-2}$	$2.01 \times 10^{-4} \text{ m}^{-2}$	-1.82%
I_5	$7.71 \times 10^{-6} \text{ m}^{-2}$	$7.95 \times 10^{-6} \text{ m}^{-2}$	-3.13%

Comparisons of simulations using the full wiggler model and the reduced MAD-style “bend-drift-bend” wiggler have shown that wiggler nonlinearities do not significantly affect the correction of optics functions or the final emittance. Therefore, the simplified “bend-drift-bend” wiggler model is used for all `ring_ma2` studies on the ILC damping ring lattice. This reduces the time required to simulate the correction procedure for one randomly-misaligned lattice by a factor of 15.

The second modification affects the process through which optics measurements are simulated. In [22], measurements are simulated on a turn-by-turn basis, applying BPM measurement errors on every turn. Simulating one betatron phase measurement requires particle tracking for over 40,000 turns, applying simulated BPM measurement errors on every turn. Even with the simplified wiggler model, this is prohibitively slow on a lattice as large as DTC04. An alternative is used in these studies where BPM errors are applied directly to the `Bmad`-computed optics functions. Although not as rigorous as the full measurement simulation method, side-by-side comparisons of the two methods have shown minimal difference in the resulting optics functions. As a result, the amount of time to simulate the correction procedure for one randomly-misaligned and corrected lattice is further reduced by another factor of 25, allowing the characterization of each configuration to be completed in a reasonable amount of time.

The optics correction procedure used in this characterization was developed at CEsrTA [22], and relies on the measurement and correction of the betatron phase and coupling [19] using beam position monitors (BPMs) with turn-by-turn capabilities [15]. The BPM modules are capable of pre-processing phase data in parallel, therefore this method has the benefit that data acquisition time is roughly independent of the number of BPMs, and is entirely independent of the number of correctors.

The correction procedure used here is as follows:

1. Measure the closed orbit. Fit the data using all 826 steering correctors (150 each of dedicated horizontal and vertical steerings, and 263 combined horizontal/vertical correctors) and apply

corrections to the lattice model.

2. Measure the betatron phase/coupling and dispersion. Correct betatron phase and horizontal dispersion to the design values using all 813 normal quadrupoles; simultaneously correct betatron coupling using all 160 skew quadrupole correctors, and apply all corrections.
3. Remeasure the closed orbit, coupling, and vertical dispersion; simultaneously correct all machine data using all 513 steering correctors and 160 skew quadrupole correctors and apply corrections.

The correction procedure described above is routinely used at CesrTA, therefore a direct comparison of simulation with measurement is available to validate the emittance tuning method. Details of the CesrTA characterization are available in [24, 22]. Although CesrTA has not achieved a vertical emittance below 2 pm as required for the ILC damping rings, simulated optics functions after correction are in agreement with measurements of the optics at CesrTA, and demonstrate accuracy in the modeling of the correction procedure. In practice, corrections based on betatron phase and coupling have yielded coupling and dispersion on par with that achieved using orbit response matrix analysis at CesrTA [23].

4. Error Tolerance of DTC04

The magnet misalignments, guide field errors, multipole errors, and BPM measurement error tolerances specified in the ILC Technical Design Report are applied in order to demonstrate that the baseline design satisfies the requirements for achieving vertical emittance. As will be seen, the full complement of BPMs is more than sufficient to achieve the requisite vertical emittance.

4.1 Nominal Lattice and Errors

Misalignments and BPM measurement error tolerances are summarized in table 7 in the Appendix, and are based on errors used in previous studies [21]. In addition, quadrupole k_1 and sextupole k_2 errors are now included. Multipole error coefficients are taken from measurements of PEP-II guide field multipole errors by Cai [5], and are summarized in table 8 in the Appendix. These error amplitudes and multipole coefficients, along with the full complement of 511 BPMs, define the nominal ILC-DR scenario.

Results of `ring_ma2` studies for this scenario are shown in figure 4 and are summarized in table 4. The coupling in model lattices is characterized using the \bar{C} coupling matrix [20], an extension of the Edwards and Teng formalism [11]. In particular, the out-of-phase coupling matrix element \bar{C}_{12} is used, as the \bar{C}_{12} measurement is insensitive to BPM rotation.

Including misalignments, guide field errors, multipole errors, and BPM measurement error tolerances, 95% of the resulting lattices have a vertical emittance below $\epsilon_b = 0.224$ pm after corrections. This is well below the emittance budget of $\epsilon_b = 2$ pm, though it is important to note that collective effects and other non-static sources of emittance dilution have not been accounted for in the calculation of the simulated emittance.

The fundamental lower limit for the vertical emittance is determined by the finite opening angle of synchrotron radiation, and for the ILC damping rings is around 0.1 pm. The zero-current

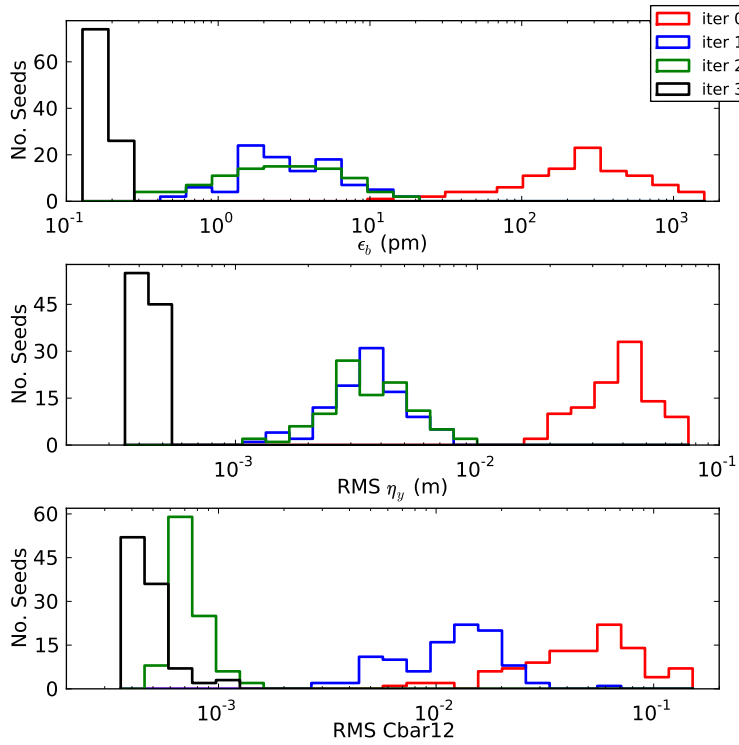


Figure 4: Distributions for emittance, dispersion, and coupling with misalignments, guide field multipole errors, and BPM errors as specified in the ILC TDR, using the full compliment of BPMs. Before correction (red), and after the first, second, and third corrections (blue, green, and black, respectively) are shown. Note that the horizontal axis is on a log-scale.

emittances achieved after correction for the nominal scenario is close to this limit, with 95% of seeds well within a factor of three of the lower bound.

4.2 Reduced BPM Schemes

It is clear that the baseline specifications for misalignments, multipole errors, and BPM and corrector distributions, as specified in the Technical Design Report, are more than sufficient to contain the static optics contribution to the vertical emittance within the 2 pm emittance budget. It is of interest to consider whether the number of BPMs can be reduced without compromising the effectiveness of the emittance correction procedure.

The ILC damping ring lattice is wiggler-dominated, with $> 80\%$ of synchrotron radiation being generated by the damping wigglers. As such, residual vertical dispersion in the wiggler straight will contribute significantly more to the vertical emittance than a comparable residual in the arcs. Preserving the 52 BPMs in the damping wiggler straight is therefore essential. The remaining 459 BPMs are either in other straight sections (159) or in the arcs (300).

The baseline arc cell design has two BPMs, indicated in figure 3. The optics functions at the two BPMs are summarized in table 5. The betatron phase advance per arc is roughly 15 (≈ 94.25 rad), corresponding to about 10 BPMs per betatron wavelength in the arcs. The large number

Table 4: 95th-percentile vertical emittance, RMS vertical dispersion, and RMS coupling after each round of corrections, for the nominal lattice defined in Sec.

Iteration	Parameter	95 th Percentile
Initial	ε_b	1010 pm
	RMS η_y	64.5 mm
	RMS \bar{C}_{12}	121×10^{-3}
$x + y$	ε_b	12.3 pm
	RMS η_y	6.37 mm
	RMS \bar{C}_{12}	23.0×10^{-3}
$\phi_{a,b} + \bar{C}_{12} + \eta_x$	ε_b	10.9 pm
	RMS η_y	6.92 mm
	RMS \bar{C}_{12}	1.11×10^{-3}
$y + \bar{C}_{12} + \eta_y$	ε_b	0.224 pm
	RMS η_y	0.502 mm
	RMS \bar{C}_{12}	0.704×10^{-3}

of BPMs and low phase advance per arc cell imply that not every BPM in the arcs may be necessary in order to maintain the ability to correct the lattice to below 2 pm vertical emittance.

Table 5: Optics functions evaluated at each of the two periodic BPM locations in the DTC04 arc cell, denoted by “odd-indexed” and “even-indexed”.

Parameter	Odd-Indexed	Even-Indexed
β_a	15.1 m	6.5 m
β_b	14.9 m	23.5 m
η_a	0.312 m	0.185 m

Five scenarios for BPM distributions are examined. They are:

1. Full complement of BPMs, for a total of 511; 10 BPMs per betatron wavelength. This is the nominal scenario from Sec. 4.1.
2. Remove odd-indexed arc BPMs, for a total of 361; 5 BPMs per betatron wavelength, at locations with $\beta_b > \beta_a$
3. Remove even-indexed arc BPMs, for a total of 361; 5 BPMs per betatron wavelength, at locations with $\beta_b \approx \beta_a$
4. Remove all odd-indexed and every other even-indexed arc BPM, for a total of 287; 2.5 BPMs per betatron wavelength, at locations with $\beta_b > \beta_a$
5. Remove all even-indexed and every other odd-indexed arc BPM, for a total of 287; 2.5 BPMs per betatron wavelength, at locations with $\beta_b \approx \beta_a$

For each BPM distribution, the misalignment and correction procedure described in Sec. 4.1 is repeated. Magnet and BPM errors are identical for the five scenarios, therefore a direct comparison of resulting corrections is possible. Correction levels achieved for lattices with these BPM distributions are shown in figure 5, and are summarized in table 6.

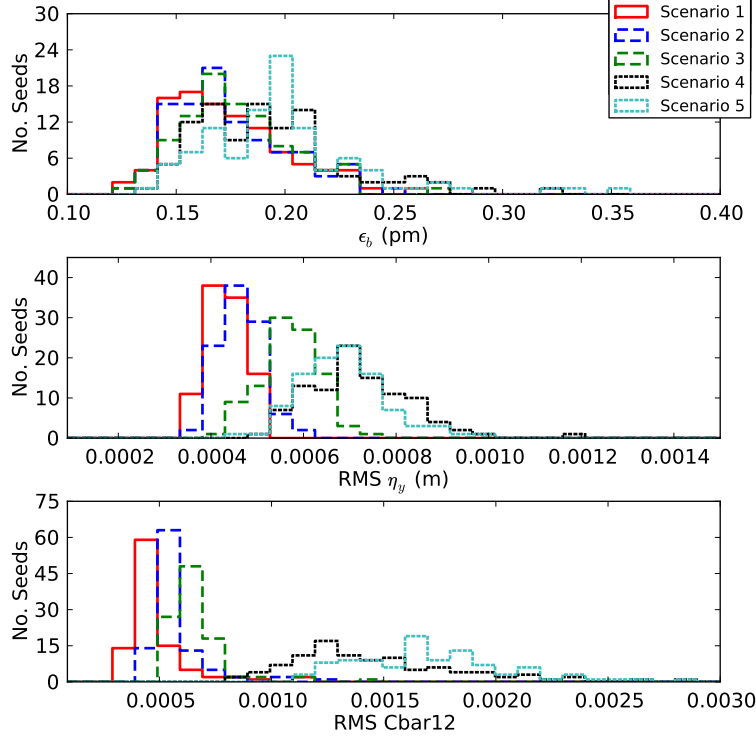


Figure 5: ϵ_b , η_y , and \bar{C}_{12} after the full correction procedure for various BPM distributions. See text for definitions of each scenario. Dashed lines indicate a scenario with 50% of arc BPMs removed; dash-dotted lines indicate a scenario with 75% of arc BPMs removed. Note that the horizontal axis is now linear.

Table 6: 95th percentile of ϵ_b , RMS η_y , and RMS \bar{C}_{12} after final correction with reduced BPM counts. See text for definitions of each BPM count scenario.

BPM Scheme	ϵ_b (pm)	RMS η_y (mm)	RMS \bar{C}_{12} (%)
Scenario 1	0.224	0.502	0.0704
Scenario 2	0.224	0.547	0.0790
Scenario 3	0.225	0.670	0.0863
Scenario 4	0.263	0.892	0.216
Scenario 5	0.269	0.838	0.239

With half of the arc BPMs removed (scenarios 2-3), the correction procedure achieves vertical emittance below 0.224-0.225pm for 95% of the lattices. With the removal of 3/4 of BPMs in the arcs (scenarios 4-5), there is a slight increase in the 95th percentile ϵ_b to 0.263-0.269 pm, still well

below the 2 pm requirement. There is a weak preference for retaining the “even-indexed” BPMs (scenarios 2 and 4) as compared to the “odd-indexed” BPMs (scenarios 3 and 5). Scenarios 3 and 5 will therefore be omitted from further discussion.

4.3 Effect of Random BPM Failures

From the proceeding discussion, it is clear that the BPM count can be reduced substantially with respect to the baseline design specification without compromising the effectiveness of the emittance tuning procedure. However, this assumes all remaining BPMs are fully functional. This is rarely the case in a real machine, and as such, the effects of random BPM failures must be explored before deeming a BPM distribution acceptable.

Again using the same random seeds as in previous simulations for generating lattice and BPM errors, a random subset of BPMs is flagged as not functional, and therefore not used in corrections. As there are multiple BPM distributions under evaluation, only the fraction of BPMs tagged as “failed” is constant between BPM distribution scenarios, rather than failing a fixed number of BPMs. The exact subset of BPMs for each test will therefore not remain the same between each BPM distribution scenario. It is not possible to have a truly random distribution of BPM failures while requiring that the same BPMs are tagged as “failed” between the three BPM distribution scenarios evaluated here, since the total number and distribution of BPMs varies from one scenario to the next. As such, BPM failure tests on each individual BPM distribution scenario are directly comparable seed-by-seed, but there is a small statistical variation between the different BPM distribution scenarios for a fixed percentage of BPM failures.

It is assumed that in practice, the damping rings would not be operated if more than 10% of BPMs have failed. In this study, the fraction of BPMs tagged as “failed” is increased from 0% to 10%. Figure 6 demonstrates the evolution of the 95th-percentile ε_b , RMS η_y , and RMS \bar{C}_{12} with respect to the fraction of failed BPMs for the nominal case (scenario 1) and BPM distributions with 1/2 and 3/4 of arc BPMs removed (scenarios 2 and 4, respectively).

The resulting emittance, dispersion, and coupling of scenarios 1 and 2 are nearly identical, within the expected statistical variation. Scenario 4, with only 1/4 of arc BPMs with respect to the baseline design, shows more rapid growth in emittance, dispersion, and coupling as the fraction of failed BPMs increases. Vertical emittance growth from intra-beam scattering will increase with vertical dispersion [12], thus making scenario 4 unattractive. It is therefore concluded that one of the two BPMs in every arc cell may be removed without affecting the robustness of the emittance tuning procedure.

5. Dynamic Aperture

After a lattice model has been misaligned and corrected using the simulated emittance tuning procedure, the dynamic aperture is evaluated through tracking. The dynamic aperture is defined as the maximum stable amplitude in the transverse plane. Trajectories with initial coordinates inside the dynamic aperture boundary will remain within that boundary for at least 1000 turns. The amplitude for trajectories with initial coordinates outside the boundary will be lost within 1000 turns. The tracking is repeated for off-energy particles to compute the energy dependence of the dynamic aperture.

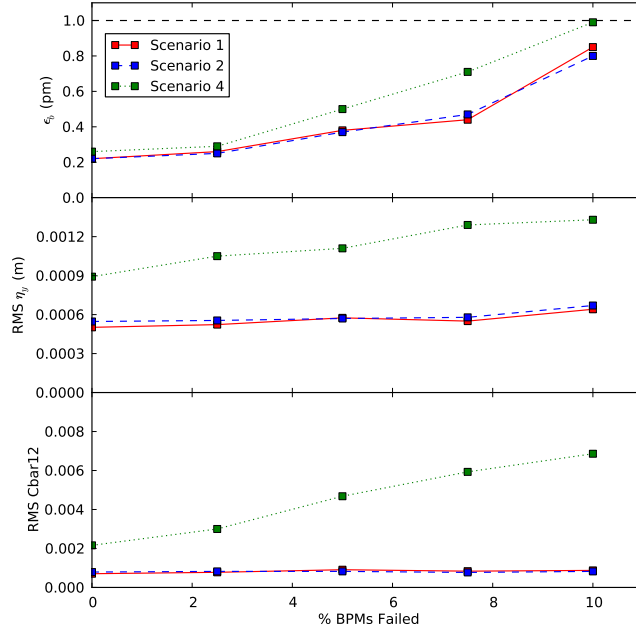


Figure 6: 95th-percentile ϵ_b , RMS η_y , and RMS \bar{C}_{12} as a function of the fraction of BPMs randomly disabled, for three potential BPM distributions. See text for definitions of each BPM distribution. The dashed black line indicates $\epsilon_b = 1$ pm.

The full wiggler map is required for evaluating the dynamic aperture in order to account for wiggler nonlinearities. This greatly increases the required computation time for a dynamic aperture study, however individual jobs are easily parallelized. Analysis has shown minimal variation of dynamic aperture between different sets of misalignments and corrections, given the same misalignment amplitudes. Therefore only one seed for each test configuration is evaluated for dynamic aperture. Here, the random seed corresponding to the 95th-percentile lattice after misalignments and correction is used.

Figure 7a shows the dynamic aperture for the nominal scenario, as defined in Sec. 4.1. It is evident that the systematic and random multipole errors as specified in the ILC Technical Design Report are more than sufficient to achieve the required dynamic aperture for accepting an incoming bunch from the positron source.

The possibility that magnet manufacturing requirements may be relaxed by increasing the tolerance on magnet multipole errors is explored. Starting with the nominal DTC04 lattice characterized in Section 4.1, both systematic and random multipole coefficients are increased by a constant multiplier from 5x-20x with respect to the values in table 8. All other misalignments and BPM measurement errors are identical to the nominal scenario. Results are shown in figures 7b–7d.

The multipole error constraints as specified in the ILC TDR are evidently over-specified by a factor of 20.

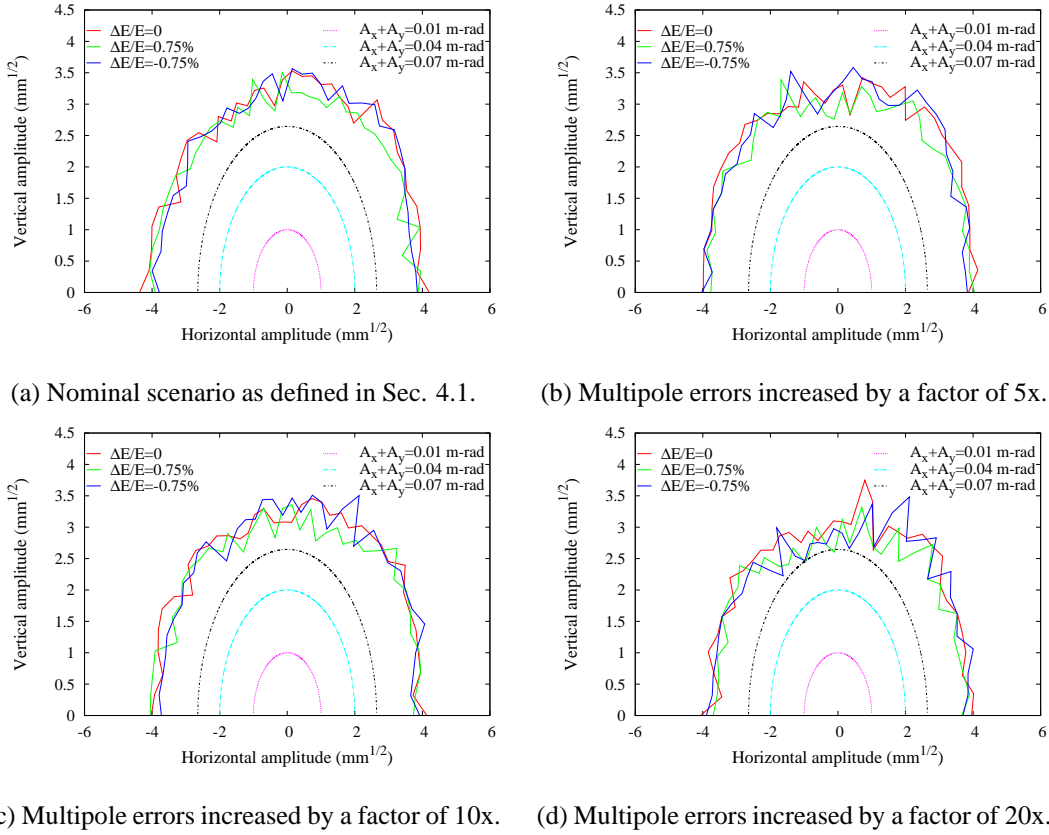


Figure 7: Dynamic aperture for the DTC04 lattice, while varying the amplitude of systematic and random multipole errors. All scenarios shown include the full complement of BPMs. The overlaid black ellipse represents the maximum expected amplitude for bunches transferred from the positron source [1].

6. Summary and Future Work

A method has been presented for determining the effectiveness of corrections for the ILC damping rings and the resulting dynamic aperture after correction, using the emittance tuning algorithm developed and used at CEsrTA. Lattice models include misaligned magnets, magnet strength and multipole errors, and BPM measurement errors. The method is versatile and may be applied to any closed lattice to evaluate the sensitivity of the effectiveness of emittance corrections to changes in BPM and corrector distributions, multipole tolerances, and more.

Based on this method, the ILC damping ring design, misalignment tolerances, and BPM measurement errors as presented in the ILC Technical Design Report (TDR) have been shown to achieve the required zero-current vertical emittance and dynamic aperture. Note that collective effects such as intra-beam scattering, electron cloud, and fast-ion instability can only increase the vertical emittance above this minimum.

One of the two BPMs in every arc cell may be removed without impact on the correction capabilities, even when accounting for up to a 10% BPM failure rate. This leaves approximately 5 BPMs per betatron wavelength in the arcs. A further reduction of BPMs in the arcs to 1/4 of the

original count (≈ 2.5 BPMs per betatron wavelength) causes a substantial increase in dispersion and coupling, subsequently fueling emittance growth from collective effects. Specifications for magnet multipole errors can be relaxed by a factor of twenty without compromising the dynamic aperture.

An infrastructure exists for evaluating further lattice modifications, such as sextupole optimizations, increased magnet or BPM errors, changes in corrector distributions, or a change in working point. Further lattice developments in these areas can therefore be easily evaluated for the ILC damping rings or any arbitrary closed lattice.

Acknowledgments

This work was supported by the National Science Foundation grant PHY-1002467 and Department of Energy grant DE-SC0006505.

Appendix: DTC04 Magnet Misalignments and Multipoles

Multipole coefficients are defined in the following way:

$$(B_y + iB_x) = B(r) \sum_{n=1} (b_n + ia_n) \left(\frac{x}{r} + i\frac{y}{r} \right)^{n-1} \quad (1)$$

where n is the multipole order, and b_n, a_n are the normal and skew components, respectively. Multipoles are evaluated at a reference radius of $r = 3$ cm for dipoles, 5 cm for quadrupoles, and 3.2 cm for sextupoles.

Table 7: Misalignments and errors introduced into the model ILC-DR lattice.

Element	Error	Amplitude	Units
Dipole	Roll	50	μrad
Quadrupole	x, y Offset	25	μm
	Tilt	50	μrad
	k1	0.1%	%
Sextupole	x, y Offset	25	μm
	Tilt	25	μrad
	k2	1%	%
Wiggler	Tilt	100	μrad
	y Offset	100	μm
BPM	Diff. Resolution	1	μm
	Abs. Resolution	50	μm
	Tilt	10	mrad
	Button Gains	0.5%	%
	Button Timing	10	ps

Table 8: Nominal multipoles (systematic and random) introduced into the model lattice. Coefficients are taken from multipole measurements by Y. Cai at PEP-II [5].

Element	Multipole	Systematic	Random
Dipole	b3	1.6×10^{-4}	8×10^{-5}
	b4	-1.6×10^{-5}	8×10^{-6}
	b5	7.6×10^{-5}	3.8×10^{-5}
Quadrupole	a3	-1.15×10^{-5}	7.25×10^{-5}
	a4	1.41×10^{-5}	1.27×10^{-4}
	a5	6.2×10^{-7}	1.62×10^{-5}
	a6	-4.93×10^{-5}	3.63×10^{-4}
	a7	-1.02×10^{-6}	6.6×10^{-6}
	a8	3.8×10^{-7}	6.6×10^{-6}
	a9	-2.8×10^{-7}	4.9×10^{-6}
	a10	-5.77×10^{-5}	2.33×10^{-4}
	a11	-3.8×10^{-7}	3.5×10^{-6}
	a12	-6.53×10^{-6}	3.66×10^{-5}
	a13	1.2×10^{-6}	8.6×10^{-6}
	a14	-7.4×10^{-7}	4.46×10^{-5}
	b3	-1.24×10^{-5}	7.61×10^{-5}
	b4	2.3×10^{-6}	1.32×10^{-4}
	b5	-4.3×10^{-6}	1.5×10^{-5}
	b6	3.4×10^{-4}	1.65×10^{-4}
	b7	3×10^{-7}	6.7×10^{-6}
	b8	6×10^{-7}	8.9×10^{-6}
	b9	6×10^{-7}	4.6×10^{-6}
	b10	-6.17×10^{-5}	2.46×10^{-4}
	b11	-2×10^{-7}	4.2×10^{-6}
b12	3.6×10^{-6}	3.48×10^{-5}	
b13	6×10^{-7}	9.2×10^{-6}	
b14	1×10^{-6}	4.76×10^{-5}	
Sextupole	b4	1×10^{-4}	1×10^{-4}
	b5	5×10^{-5}	3×10^{-5}
	b6	3.5×10^{-4}	1×10^{-4}
	b7	5×10^{-5}	3×10^{-5}
	b8	5×10^{-5}	3×10^{-5}
	b9	5×10^{-5}	3×10^{-5}
	b10	5×10^{-5}	3×10^{-5}
	b11	5×10^{-5}	3×10^{-5}
	b12	1.6×10^{-3}	1×10^{-4}
	b13	5×10^{-5}	3×10^{-5}
	b14	5×10^{-5}	3×10^{-5}

References

- [1] *The International Linear Collider Technical Design Report*, Tech. report, ILC Global Design Effort, 2013.
- [2] M. Aiba, M. Böge, J. Chrin, N. Milas, T. Schilcher, and A. Streun, *Comparison of linear optics measurement and correction methods at the swiss light source*, Phys. Rev. ST Accel. Beams **16** (2013), 012802.
- [3] M. Aiba, M. Boge, N. Milas, and A. Streun, *Ultra low vertical emittance at SLS through systematic and random optimization*, Nucl. Instrum. Methods Phys. Res. A **694**.
- [4] C. Baumgarten, *Geometrical method of decoupling*, Phys. Rev. ST Accel. Beams **15** (2012), 124001.
- [5] Y. Cai, *Measured Multipole Errors in PEP-II and SPEAR3 Magnets*, Tech. report, SLAC, 2005.
- [6] P. Castro, J. Borer, A. Burns, G. Morpurgo, and R. Schmidt, *Betatron function measurement at LEP using the BOM 1000 turns facility*, Proceedings of the 1993 Particle Accelerator Conference **3** (1993), 2103–2105.
- [7] J. A. Crittenden, A. Mikhailichenko, E. Smith, K. Smolenski, and A. Temnykh, *Field Modeling for the CESR-C Superconducting Wiggler Magnets*, Proceedings of the 2005 Particle Accelerator Conference, Knoxville, TN, 2005, pp. 2336–2338.
- [8] J. A. Crittenden, M. A. Palmer, and D. L. Rubin, *Wiggler Magnet Design Development for the ILC Damping Rings*, Proceedings of the 2012 International Particle Accelerator Conference, New Orleans, LA, 2012, pp. 1969–1971.
- [9] R. Dowd, M. Boland, G. LeBlanc, and Y-R. E. Tan, *Achievement of Ultralow Emittance Coupling in the Australian Synchrotron Storage Ring*, Phys. Rev. ST Accel. Beams **14**.
- [10] G. F. Dugan, M. A. Palmer, and D. L. Rubin, *ILC Damping Rings R&D at CEsrTA*, ICFA Beam Dynamics Newsletter (J. Urakawa, ed.), no. No. 50, International Committee on Future Accelerators, December 2009, pp. 11–33.
- [11] D. Edwards and L. Teng, *Parametrization of Linear Coupled Motion in Periodic Systems*, IEEE Trans. Nucl. Sci **20** (1973).
- [12] M. P. Ehrlichman, W. Hartung, B. Heltsley, D. P. Peterson, N. Rider, D. Rubin, D. Sagan, J. Shanks, S. T. Wang, R. Campbell, and R. Holtzapple, *Intrabeam scattering studies at the cornell electron storage ring test accelerator*, Phys. Rev. ST Accel. Beams **16** (2013), 104401.
- [13] A. Franchi, L. Farvacque, J. Chavanne, F. Ewald, B. Nash, K. Scheidt, and R. TomáÅs, *Vertical emittance reduction and preservation in electron storage rings via resonance driving terms correction*, Physical Review Special Topics - Accelerators and Beams **14** (2011), no. 3 (en).
- [14] M. Korostelev and A. Wolski, *DCO4 Lattice Design for 6.4 km ILC Damping Rings*, Proceedings of the 2010 International Particle Accelerator Conference, Kyoto, Japan, 2010, pp. 3575–3577.
- [15] M. A. Palmer et al., *CESR Beam Position Monitor System Upgrade for CEsrTA and CHESSE Operations*, Proceedings of the 2010 International Particle Accelerator Conference, Kyoto, Japan, 2010, pp. 1191–1193.
- [16] Hong Qin, Ronald C. Davidson, Moses Chung, and Joshua W. Burby, *Generalized courant-snyder theory for charged-particle dynamics in general focusing lattices*, Phys. Rev. Lett. **111** (2013), 104801.

- [17] J. Safranek, G. Portmann, A. Terebilo, and C. Steier, *MATLAB-Based LOCO*, Tech. report, SSRL/SLAC and LBNL, 2002.
- [18] D. Sagan, *Bmad: A Relativistic Charged Particle Simulation Library*, Nucl. Instrum. Methods Phys. Res. **A558** (2006), 356–359.
- [19] D. Sagan, R. Meller, R. Littauer, and D. Rubin, *Betatron Phase and Coupling Measurements at the Cornell Electron/Positron Storage Ring*, Phys. Rev. ST Accel. Beams **3** (2000).
- [20] D. Sagan and D. Rubin, *Linear Analysis of Coupled Lattices*, Phys. Rev. ST Accel. Beams **2** (1999).
- [21] J. Shanks and D. Rubin, *ILC Damping Ring Lattice Error Tolerances*, 2012 International Workshop on Future Linear Colliders, Arlington, TX, 2012.
- [22] J. Shanks, D.L. Rubin, and D. Sagan, *Low-emittance tuning at the cornell electron storage ring test accelerator*, Phys. Rev. ST Accel. Beams **17** (2014), 044003.
- [23] J. P. Shanks et al., *CesrTA Low-Emittance Tuning—First Results*, Proceedings of the 2009 Particle Accelerator Conference, Vancouver, BC, 2009, pp. 2754–2756.
- [24] James Shanks, *Low-Emittance Tuning at CesrTA*, Ph.D. thesis, Cornell University, Ithaca, New York, 2013.
- [25] Andrzej Wolski, *Alternative approach to general coupled linear optics*, Phys. Rev. ST Accel. Beams **9** (2006), 024001.